Neural mechanism for binaural pitch perception via ghost stochastic resonance

Pablo Balenzuela[a] and Jordi García-Ojalvo[b]
Departament de Física e Enginyeria Nuclear, Universitat Politècnica de Catalunya, Colom 11, E-08222 Terrassa, Spain

(Received 3 September 2004; accepted 26 January 2005; published online 15 April 2005)

We present a physiologically plausible binaural mechanism for the perception of the pitch of complex sounds via ghost stochastic resonance. In this scheme, two neurons are driven by noise and a different periodic signal each (with frequencies $f_1=kf_0$ and $f_2=(k+1)f_0$, where $k>1$), and their outputs (plus noise) are applied synaptically to a third neuron. Our numerical results, using the Morris–Lecar neuron model with chemical synapses explicitly considered, show that intermediate noise levels enhance the response of the third neuron at frequencies close to f_0, as in the cases previously described of ghost resonance. For the case of an inharmonic combination of inputs ($f_1=kf_0+\Delta f$ and $f_2=(k+1)f_0+\Delta f$) noise is also seen to enhance the rates of most probable spiking for the third neuron at a frequency $f_r=f_0+[\Delta f/(k+1/2)]$. In addition, we show that similar resonances can be observed as a function of the synaptic time constant. The suggested ghost-resonance-based stochastic mechanism can thus arise either at the peripheral level or at a higher level of neural processing in the perception of pitch. © *2005 American Institute of Physics*.
[DOI: 10.1063/1.1871612]

The perception and processing of environmental complex signals resulting from the combination of multiple inputs is a nontrivial task for the nervous system. In many species, solving efficiently this sensory problem could have an evolutionary payoff. A classical example is the perception of the pitch of complex sounds by the auditory system, the mechanism of which remains controversial. Recently, a mechanism for the perception of pitch has been proposed on the basis of the so-called ghost stochastic resonance. Under this paradigm, an appropriate level of noise yields an optimal subharmonic neural response to a combination of two or more harmonic signals that lack the fundamental frequency, which is nevertheless perceived by the system. The original proposal concentrated in the peripheral level of the perception process, by considering the case of a simple monoaural presentation of the complex signal. On the other hand, it is known that complex sounds are also perceived when its two constituent tones are presented binaurally (i.e., one in each ear). Thus, the question that remains is whether ghost stochastic resonance can participate in detecting this "virtual" dichotic pitch at a higher level of processing. In this paper we present, on the basis of numerical simulations, a plausible mechanism for the binaural perception of the pitch of complex signals via ghost stochastic resonance. In this scenario, each of the two input tones drives a different noisy neuron (corresponding to detection in the left–right auditory pathways), and together they drive a third noisy neuron that perceives the missing fundamental. In this way, the same basic mechanism of ghost resonance can explain pitch perception occurring at both the peripheral and a higher processing level.

I. INTRODUCTION

A. Pitch perception by single neurons

Under many conditions sensory neurons can be considered as noisy threshold detectors, responding to external signals (either from the environment or from other neurons) in an all-or-nothing manner. Substantial effort has been dedicated to examine theoretically and numerically the response of neurons to simple input signals, usually harmonic, both under deterministic[1,2] and stochastic[3,4] conditions.

Much less studied is the case of multiple input signals. It is known, for instance, that a high-frequency signal enhances the response of a neuron to a lower frequency driving via vibrational resonance.[5] On the other hand, two-frequency signals are commonly used for diagnostic purposes, such as in the analysis of evoked potentials in the human visual cortex,[6] but the detection and processing of this type of combined signals is poorly understood. Recently, a study of the response of a neuron to a combination of harmonics in which the fundamental is missing[7] has shed new light upon the problem of the perception of the pitch of complex sounds.[8]

The perceived pitch of a pure tone is simply its frequency. In contrast, the perceived pitch of a complex sound (formed by a combination of pure tones) is a subjective attribute, which can nevertheless be quantified accurately by comparing it with a pure tone. In the particular case of harmonic complex sounds (signals whose constituent frequencies are multiple integers of a fundamental frequency), the perceived pitch is the fundamental, even if that frequency is not spectrally present in the signal. For that reason, the pitch

[a]Also at: Departamento de Física, FCEyN, Universidad de Buenos Aires, Pabellón 1, Ciudad Universitaria (1428), Buenos Aires, Argentina. Electronic mail: pablo.balenzuela@upc.edu
[b]Electronic mail: jordi.g.ojalvo@upc.es

is usually referred to in this case as a "virtual pitch," and its perception is sometimes called the "missing fundamental illusion."

The neural mechanism underlying pitch perception remains controversial. From a neurophysiological perspective, the perceived pitch is associated with the inter-spike interval statistics of the neuronal firings.[9,10] The analysis presented in Refs. 7 and 8 shows that a neuron responds optimally to the missing fundamental of a harmonic complex signal for an intermediate level of noise, making use of two ingredients: (i) A linear interference of the individual tones, which naturally leads to signal peaks at the fundamental frequency, and (ii) a nonlinear threshold that detects those peaks (with the help of a suitable amount of noise, provided the signal is deterministically subthreshold). The behavior of this relatively simple model yields remarkably good agreement with previous psychophysical experiments.[11] The phenomenon has been termed *ghost stochastic resonance* (GSR), and has been replicated experimentally in excitable electronic circuits[12] and lasers.[13]

B. Signal integration and processing of distributed inputs

Besides the question of *how* pitch is perceived, another contested debate relates to *where* perception takes place. Although interval statistics of the neuronal firings[9,10] show that pitch information exists in peripheral neurons, other results seem to indicate that, at least to some extent, pitch perception takes place at a higher level of neuronal processing.[14] A typical example is found in binaural experiments, in which two components of a harmonic complex signal enter through different ears. It is known that in that case a (rather weak) low-frequency pitch is perceived. This is called "dichotic pitch," and can also arise from the binaural interaction between broad-band noises. For example, Cramer and Huggins[15] studied the effect of a dichotic white noise when applying a progressive phase shift across a narrowband of frequencies, centered on 600 Hz, to only one of the channels. With monaural presentation listeners only perceived noise, whereas when using binaural presentation over headphones, listeners perceived a 600 Hz tone against a background noise.

It is worth examining whether the ghost resonance mechanism introduced by Chialvo *et al.*[7,8] can also account for the binaural effects described above. Ghost resonance has already been seen to be enhanced by coupling in experiments with diffusively coupled excitable lasers,[16] but no studies in synaptically coupled neurons have been made so far. Given that chemical synapses lead to pulse coupling, a reliable coincidence detection is required in order for ghost resonance to arise in this case. We examine the situation in which two different neurons receive one single component of the complex signal each (so that each neuron represents detection at a different auditory channel in a binaural presentation), and act upon a third neuron which is expected to perceive the pitch of the combined signal. Our results show that this higher-level neuron is indeed able to perceive the pitch, hence providing a neural mechanism for the binaural experiments.

II. MODEL DESCRIPTION

A. Neuron model

We describe the dynamical behavior of the neurons with the Morris–Lecar model[17]

$$\frac{dV_i}{dt} = \frac{1}{C_m}(I_i^{\mathrm{app}} - I_i^{\mathrm{ion}} - I_i^{\mathrm{syn}}) + D_i\xi(t), \tag{1}$$

$$\frac{dW_i}{dt} = \phi\Lambda(V_i)[W_\infty(V_i) - W_i], \tag{2}$$

where V_i and W_i stand for the membrane potential and the fraction of open potassium channels, respectively, and the subindex i labels the different neurons, with $i=1,2$ representing the two input neurons and $i=3$ denoting the processing neuron. C_m is the membrane capacitance per unit area, I_i^{app} is the external applied current, I_i^{syn} is the synaptic current, and the ionic current is given by

$$I_i^{\mathrm{ion}} = g_{Ca}M_\infty(V_i)(V_i - V_{Ca}^0) + g_K W_i(V_i - V_K^0) + g_L(V_i - V_L^0), \tag{3}$$

where $g_a(a=Ca,K,L)$ are the conductances and V_a^0 the resting potentials of the calcium, potassium and leaking channels, respectively. The following functions of the membrane potential are also defined:

$$M_\infty(V) = \frac{1}{2}\left[1 + \tanh\left(\frac{V - V_{M1}}{V_{M2}}\right)\right], \tag{4}$$

$$W_\infty(V) = \frac{1}{2}\left[1 + \tanh\left(\frac{V - V_{W1}}{V_{W2}}\right)\right], \tag{5}$$

$$\Lambda(V) = \cosh\left(\frac{V - V_{W1}}{2V_{W2}}\right), \tag{6}$$

where V_{M1}, V_{M2}, V_{W1}, and V_{W2} are constants to be specified later. The last term in Eq. (1) is a white noise term of zero mean and amplitude D_i, uncorrelated between different neurons.

In the deterministic and single-neuron case, this system shows a bifurcation to a limit cycle for increasing applied current I^{app}.[18] This bifurcation can be a saddle-node (type I) or a subcritical Hopf bifurcation (type II) depending on the parameters. We chose this last option for the numerical calculations presented in this paper (It is currently not known what type of neurons detect the pitch in the auditory system. However, our investigations on standard stochastic resonance show that the response of both types of neurons to single-frequency driving is qualitative identical,[19] so we can expect that the results to be described below will also hold in type I neurons).

The specific values of the parameters used in what follows are shown in Table I.[20] The equations were integrated using the Heun method,[22] which is equivalent to a second-order Runge–Kutta algorithm for stochastic equations.

TABLE I. Parameters values of the Morris–Lecar and synapse models used in this work.

Parameters	Morris–Lecar (TII)
C_m	5 μF/cm^2
g_K	8 μS/cm^2
g_L	2 μS/cm^2
g_{Ca}	4.4 μS/cm^2
V_K	−80 mV
V_L	−60 mV
V_{Ca}	120 mV
V_{M1}	−1.2 mV
V_{M2}	18 mV
V_{W1}	2 mV
V_{W2}	30 mV
ϕ	1/25 s^{-1}
Parameters	**Synapses**
α	0.5 ms^{-1} mM^{-1}
β	0.1 ms^{-1}
g_{syn}	(specified in each case)
τ_{syn}	(specified in each case)
E_s	0 mV

B. Synapses model

In this work we couple the neurons using a simple model of chemical synapses.[21] In this model, the synaptic current through neuron i is given by

$$I_i^{\text{syn}} = \sum_{j \in \text{neigh}(i)} g_i^{\text{syn}} r_j (V_i - E_s), \tag{7}$$

where the sum runs over the neighbors that feed neuron i, g_i^{syn} is the conductance of the synaptic channel, r_j stands for the fraction of bound receptors of the postsynaptic channel, V_i is the postsynaptic membrane potential, and E_s is a parameter whose value determines the type of synapses (if larger than the rest potential, e.g., $E_s = 0$ mV, the synapses is excitatory; if smaller, e.g., $E_s = -80$ mV, it is inhibitory).

The fraction of bound receptors, r_i, follows the equation:

$$\frac{dr_i}{dt} = \alpha [T]_i (1 - r_i) - \beta r_i, \tag{8}$$

where $[T]_i = \theta(T_0^i + \tau_{\text{syn}} - t)\,\theta(t - T_0^i)$ is the concentration of neurotransmitter released in the synaptic cleft, α and β are rise and decay time constants, respectively, and T_0^i is the time at which the presynaptic neuron (labeled now i) fires, what happens whenever the presynaptic membrane potential exceeds a predetermined value, in our case chosen to be 10 mV. The time during which the synaptic connection is active is given by τ_{syn}. The values of the parameters that we use were taken from Ref. 21, and are specified in Table I.

III. THE CASE OF DISTRIBUTED HARMONIC COMPLEX SIGNALS

As mentioned above, we consider a network of three neurons organized in two layers. The first layer is composed of two units (called "input neurons") that receive the external inputs, and whose responses act upon the processing layer, composed in this case of only one unit (called "processing neuron"). The coupling is unidirectional from each of the input neurons to the processing neuron. Of course, physiological realism dictates that more than three neurons will be present. However, we model here for simplicity the simplest possible case; one can expect that adding more neurons will only improve the results.

In order to analyze the global response of this network to a distributed complex signal, we apply to each one of the input neurons a periodic external current with frequencies f_1 and f_2,

$$I_i^{\text{app}} = I_{0i}^{\text{app}} + A_i \cos(2\pi f_i t), \quad i = 1,2, \tag{9}$$

where the values of the bias currents I_{0i}^{app}, the modulation amplitudes A_i and the frequencies f_i will be specified below in each case.

In response to this driving, the input neurons emit a sequence of spikes with inter-spike interval (ISI) distributions centered at f_1 and f_2 and with standard deviations directly related to the noise amplitudes D_1 and D_2. The current ap-

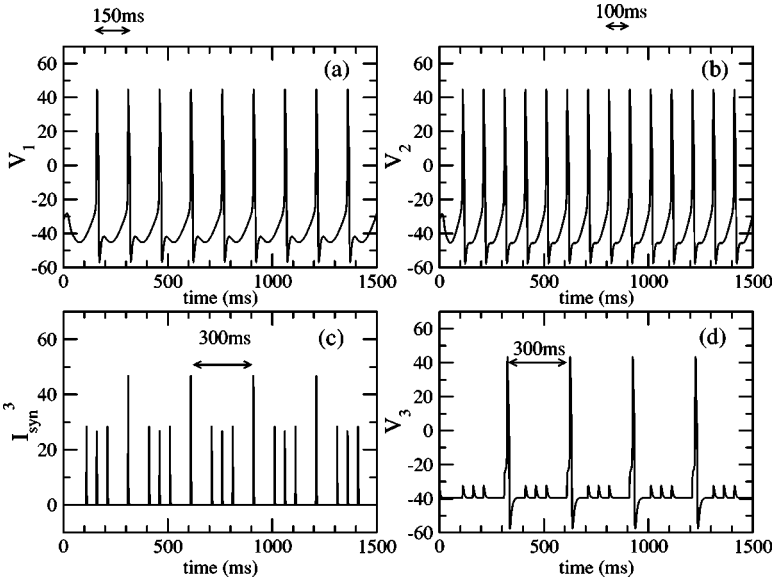

FIG. 1. Deterministic response to a distributed harmonic complex signal. The membrane potential for the three neurons is shown: (a) and (b) Input neurons, (d) processing neuron. The synaptic current acting on neuron 3, I_3^{syn}, is shown in plot (c). The two input neurons are fed with two sinusoidal signals of amplitudes $A_1 = 8$ mA, $A_2 = 8.5$ mA, and periods $T_1 = 150$ ms, $T_2 = 100$ ms, respectively (which gives a ghost resonance of $T_0 = 300$ ms). The bias current for all three neurons is $I_{0i}^{\text{app}} = 33$ mA, the synaptic coupling between input and processing neurons is $g_{\text{syn}} = 2$ nS and $\tau_{\text{syn}} = 1$ ms. All noise amplitudes are zero, $D_1 = D_2 = D_3 = 0$ mV/ms.

plied to the processing neuron is not modulated and its value, I_{03}^{app}, is also chosen below threshold, so that the neuron does not fire in the absence of synaptic coupling.

A. Deterministic case

In order to tune the system, we start the analysis in the deterministic case. Figure 1 shows the behavior of the system in the absence of noise ($D_1=D_2=D_3=0$ mV/ms). In this deterministic situation, the input neurons fire exactly with the frequencies at which they are modulated. If $f_1=kf_0$ (or, equivalently, $T_1=T_0/k$, where T_i is the period corresponding to the frequency f_i) and $f_2=(k+1)f_0$ (or $T_2=T_0/(k+1)$), the two input neurons exhibit simultaneous spikes at intervals $T_0=1/f_0$ (provided the two harmonic signals are in phase), so that the synaptic current acting on the third neuron has maxima with the same frequency, as can be observed in Fig. 1(c). In this example $T_1=150$ ms and $T_2=100$ ms, so that $k=2$ and $T_0=300$ ms. Under these conditions, and for an adequate (i.e., large enough) value of the coupling strength g_{syn}, the processing neuron fires with frequency $f_0=(1/300)$ kHz, as shown in Fig. 1(d). We can see here that the basic mechanism involved in this behavior is the detection of coincidences of incoming spikes by the output neuron. This is not entrainment nor phase locking, because that third neuron is not in the oscillatory regime, and hence it does not have a free-running frequency.

B. Stochastic case

The previous example is, however, unrealistic since in normal conditions a neuron is affected by a substantial level of noise coming from, among other sources, the background activity of other neurons acting upon it. To simulate this behavior, we add noise to the super-threshold modulation currents of the input neurons, and to the (constant) sub-threshold current of the processing neuron. We consider the three noise sources independent of each other, because the three neurons are not subject to the same background noise (they are spatially distant from each other, and in any case their synaptic connections to other neurons, main origin of the noise, will be different from each other). However, we have checked that the behavior to be presented below also holds in the case of common noise (results not shown).

Noise causes a drift in the spike times and a broadening in the distribution of ISIs [see Fig. 2(a)]. As a consequence of this, a fraction of the pulses reaching the output neuron at the ghost frequency will not do it at the same time, and the response of the processing neuron will be poorer than in the deterministic case. We will now show that even in this case the missing fundamental frequency can be successfully detected, as was suggested in Refs. 7 and 8 for a single neuron. Here the synaptic coupling g_{syn} and the applied current in the output neuron I_3^{app} are slightly below the bifurcation threshold, so that this neuron would not fire in absence of noise (when $D_3=0$ mV/ms).

With this in mind, we conduct a series of numerical experiments looking for the occurrence of ghost stochastic resonance. We choose $f_1=2$ Hz and $f_2=3$ Hz, so the ghost resonance should be located at $f_0=1$ Hz. The values of the

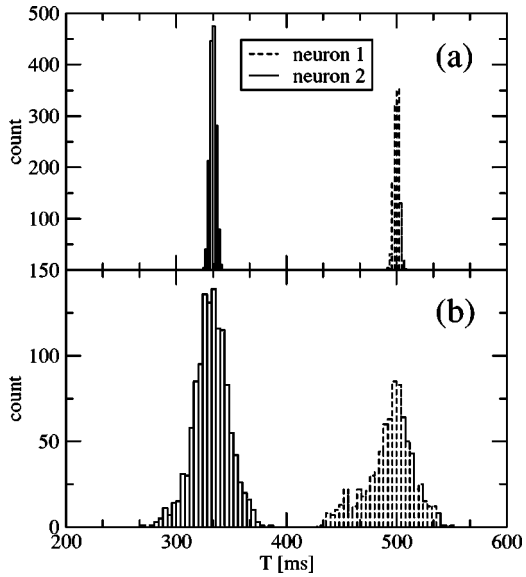

FIG. 2. Distribution of inter-spike intervals of the input neurons in two cases: (a) Both neurons with super-threshold modulation ($A_1=23.60$ mA, $A_2=24.20$ mA) plus noise ($D_1=0.05$ mV/ms, $D_2=0.2$ mV/ms); and (b) both neurons modulated with a sub-threshold harmonic current ($A_1=23.04$ mA, $A_2=22.20$ mA) plus optimal noise ($D_1=0.4$ mV/ms, $D_2=1.2$ mV/ms), i.e., in the stochastic resonance regime. The bias currents are $I_{01,2}^{app}=25$ mA and $I_{03}^{app}=2.20$ mA.

amplitudes of the modulating currents and the noise in the input neurons are those specified in Fig. 2(a). As usual in neurophysiology, in order to quantify the behavior of the system we evaluate the time between consecutive spikes, T_p. In what follows, we analyze the first two moments of the distribution of T_p, namely its mean value $\langle T_p\rangle$ and its normalized standard deviation (also known as coefficient of variation) $R_p=\sigma_p/\langle T_p\rangle$. To estimate the coherence of the output with the frequencies of interest, we also compute the fraction f_{t0} of inter-spike intervals in the neighborhood of $T_0=1/f_0$. The dependence of these variables (corresponding to the processing neuron) on the noise amplitude D_3 is shown in Fig. 3 for the case where the input neurons fire with inter-spike intervals with the distribution shown in Fig. 2(a). These results display a clear resonance at $D_3\sim 4$ mV/ms. The normalized standard deviation of the ISI distribution [Fig. 3(b)] exhibits a minimum when the spikes of the third neuron are spaced, on average, $\langle T_p\rangle=1000$ ms [Fig. 3(a)]. Additionally, around 80% of the spikes are spaced ±5% around $T_0=1000$ ms for $D_3\sim 4$ mV/ms [Fig. 3(c)]. These results clearly indicate that noise enhances the response of the processing neuron at the frequency f_0, which is not present in the input neurons.

The right panels of Fig. 3 show the probability distribution functions of the inter-spike intervals T_p for three values of the noise in the processing neuron. For low noise amplitude, the neuron spikes most likely when two input spikes arrive together, but with randomly one or more of these coincidence events is skipped. For this reason, the probability distribution function shows peaks centered at multiples of T_0, as it usually happens in conventional stochastic resonance.[23] As the noise level increases skips occurs less frequently, until an optimal noise for which almost all spikes occur every T_0,

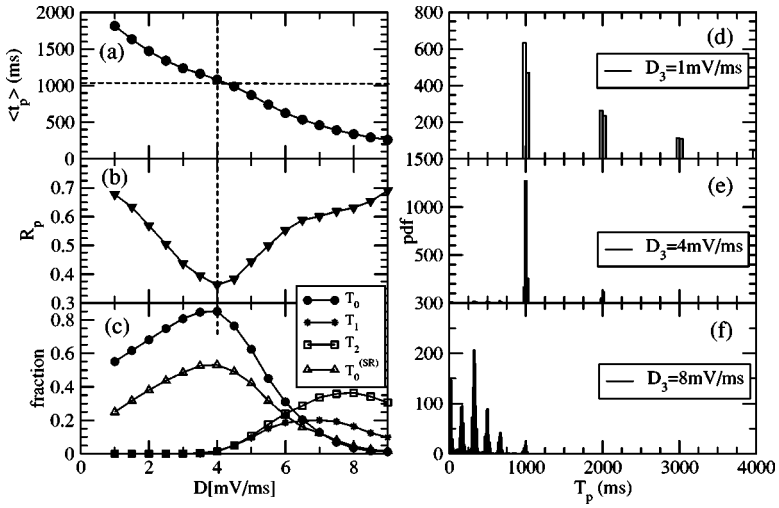

FIG. 3. Left panels: Response of the processing neuron for increasing noise amplitude: (a) Mean time between spikes $\langle T_p \rangle$, (b) coefficient of variation $R_p = \sigma_p / \langle T_p \rangle$, and (c) fraction of pulses spaced around $T_0 = 1/f_0$, $T_1 = 1/f_1$ and $T_2 = 1/f_2$ as a function of the noise amplitude in the processing neuron, D_3. Right panels: Probability distribution functions of the time between spikes T_p for three values of the noise amplitude D_3: (d) $D_3 = 1$ mV/ms, (e) $D_3 = 4$ mV/ms, and (f) $D_3 = 8$ mV/ms. Parameters are $\tau_{syn} = 35$ ms and $g_{syn} = 1$ mS for the synapses and we used $f_1 = 2$ Hz, $f_2 = 3$ Hz (which gives $f_0 = 1$ Hz). Other parameters are those of Fig. 2(a), except for the triangles in plot (c), which correspond to Fig. 2(b).

i.e., at the missing fundamental frequency. For even larger noise amplitude spikes appear at the original input periods $T_1 = 1/f_1$ and $T_2 = 1/f_2$ and at all period differences [Fig. 3(f)], as can be expected if most local maxima in the synaptic current produce a spike. The different heights of the peaks in the distribution can be understood from the fact that neurons respond differently depending on the frequency.[1]

C. Quantifying the coherence detection efficiency

As we said above, the pitch detection mechanism depends on how efficient the output neuron is in detecting the coincidences in the arriving pulses. In order to examine this issue in more detail, we have considered two ways in which coincidence detection is compromised, and measured the efficiency with which the ghost frequency is detected therein.

First, we consider the case where the modulation currents of the input neurons are sub-threshold (i.e., the neurons do not fire in absence of noise) and we add an optimal amount of noise to tune them into stochastic resonance conditions. This means that the neurons respond preferentially at their corresponding driving frequencies (again f_1 and f_2), but this firing is induced by noise, so that the corresponding ISI distributions [see Fig. 2(b)] are much broader than in the case described earlier [see Fig. 2(a)], where modulations were super-threshold, and the only role of the noise was to broaden slightly the ISI distributions. Fluctuations in the inter-spike intervals are tantamount to random phase differences between the modulated input currents. In that situation the coherence detection mechanism decreases its efficiency, as shown in Fig. 3(c): The optimal (i.e., maximal) fraction of pulses spaced at around the ghost resonance period decreases from its previous value $\gtrsim 80\%$ [full circles in Fig. 3(c)] down to $\sim 55\%$ [empty triangles in Fig. 3(c)]. Still, we note that even in this highly extreme noisy situation the ghost resonance is sufficiently detected.

In order to quantify the limit of robustness of the coherence detection mechanism, we now consider a second situation, in which a constant phase difference is added to the modulating current of neuron 2 with respect to that of neuron 1

$$I_2^{\mathrm{app}} = I_{02}^{\mathrm{app}} + A_2 \cos\left[2\pi \left(\frac{t}{T_2} + \frac{\Delta T}{T_2} \right) \right]. \tag{10}$$

Figure 4 plots the optimal fraction of pulses around the ghost resonance as a function of this phase difference, measured in terms of the timing mismatch ΔT. We set the parameters of the input neurons back into the noisy limit-cycle operation regime shown in Fig. 2(a) (super-threshold modulation plus noise). The case $\Delta T = 0$ is the one plotted in Fig. 3, where the optimal fraction of pulses around the ghost resonance is larger than 80%. As the phase difference increases that optimal fraction decreases, dropping to half its initial value for a relative timing mismatch on the order of 7.5%. This cut-off value will depend on how far below threshold the processing neuron operates, on the noise amplitude, and on the width of the ISI distributions of the input neurons [Fig. 2(a)].

D. Role of synaptic coupling

In the binaural mechanism of ghost stochastic resonance described above, synaptic coupling obviously plays an important role, since the transfer of the input modulation from the sensory neurons to the processing neuron occurs synap-

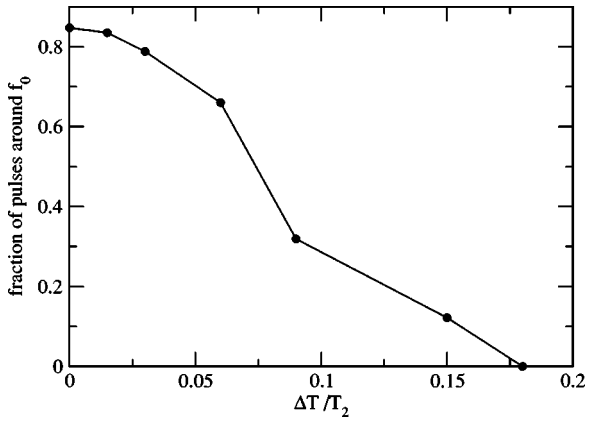

FIG. 4. Maximum fraction of pulses at the ghost resonance as a function of the timing mismatch between the input modulating currents relative to the period of the current T_2, $\Delta T / T_2$. Parameters are the same than in Fig. 3 with $D_3 = 4$ mV/ms.

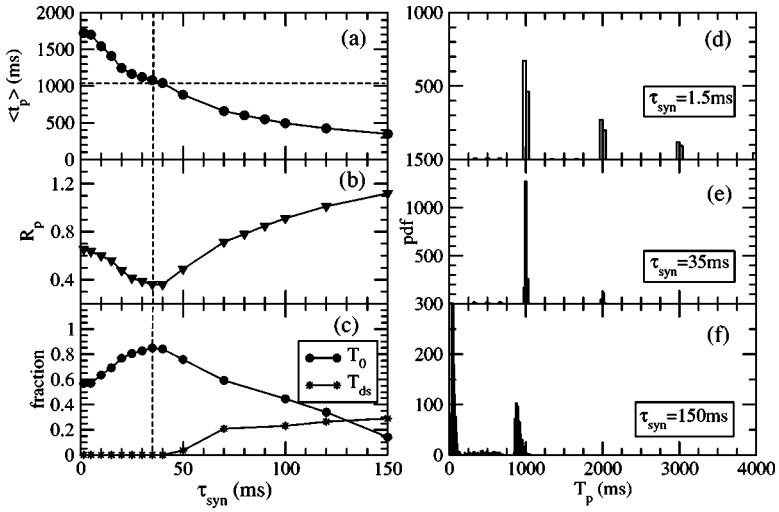

FIG. 5. Left panels: (a) Mean time between spikes, (b) coefficient of variation, and (c) fraction of pulses around $T_0=1/f_0$ and $T_{ds}=1/f_{ds}$ as a function of τ_{syn}. Right panels: Probability distribution functions of the inter-spike intervals T_p for three values of τ_{syn}: (d) $\tau_{syn}=1.5$ ms, (e) $\tau_{syn}=35$ ms, and (f) $\tau_{syn}=150$ ms. The value of g_{syn} is different for each value of τ_{syn}, chosen so that the processing neuron is below threshold and does not fire in the absence of noise. In particular, $g_{syn}=2.50$ nS for $\tau_{syn}=1.5$ ms, and $g_{syn}=1.00$ nS for $\tau_{syn}=35$ ms and $\tau_{syn}=150$ ms. The driving frequencies are $f_1=2$ Hz and $f_2=3$ Hz (which gives $f_0=1$ Hz). Other parameters are those of Fig. 3(e) (in particular, $D_3=4$ mV/ms).

tically. Taking into account that synaptic transmission is an intrinsically dynamical phenomenon (whose temporal behavior we are modeling explicitly), it is natural to expect that the characteristic time scale of this process will influence the occurrence of the resonance. Indeed, the results shown above correspond to an optimal value of the synaptic time τ_{syn}. As shown in Fig. 5 for fixed noise strength D_3, a resonance in the response of the system to the missing fundamental is also observed with respect to τ_{syn}.

We recall that τ_{syn} represents the time during which the neurotransmitters remain in the synaptic cleft before they start to disappear with rate β, and it is a measure of the width of the pulses of the synaptic current received by the processing neuron. Therefore, for low τ_{syn} [Fig. 5(d)] the synaptic pulses are very narrow, and hence coincidence detection is compromised. The characteristic probability distribution function in this case presents peaks at multiples of T_0, indicating that even if the noise level is optimized, coincident spikes from input neurons are skipped.

As τ_{syn} increases the current pulses widen and coincidence detection improves, so that an optimal situation is reached for which the ghost resonance is very clear. But if we continue increasing the value of τ_{syn} the synaptic pulses become exceedingly wide and sequences of double spikes appear (spaced by $T_{ds}=1/f_{ds}$). This happens because noise can excite two spikes while the synaptic current remains high. Indeed, Fig. 5(c) shows that the fraction of spikes occurring at intervals around T_{ds} ($\pm 5\%$) begins to be important for $\tau_{syn}>50$ ms. The corresponding distribution function in Fig. 5(f), shown here for $\tau_{syn}=150$ ms, corroborates this fact.

The joint effect of the synaptic time τ_{syn} and the noise strength D_3 can be observed in the three-dimensional plots shown in Fig. 6. This figure shows R_p and f_{t0} as a function of both D_3 and τ_{syn}. We can see the response of the processing neuron at the missing fundamental is most favorable when both parameters are simultaneously optimized. The normalized standard deviation of the ISI distribution, R_p, shows a clear minimum for $\tau_{syn}\sim 35$ ms and $D\sim 4$ mV/ms. For these same parameter values, the fraction of spikes f_{t0} occurring at intervals around T_0 exhibits a maximum at almost 80%.

IV. THE INHARMONIC CASE

A paradigmatic experimental result in pitch perception refers to the pitch reported by human subjects to the presentation of an inharmonic complex sound, in which the origi-

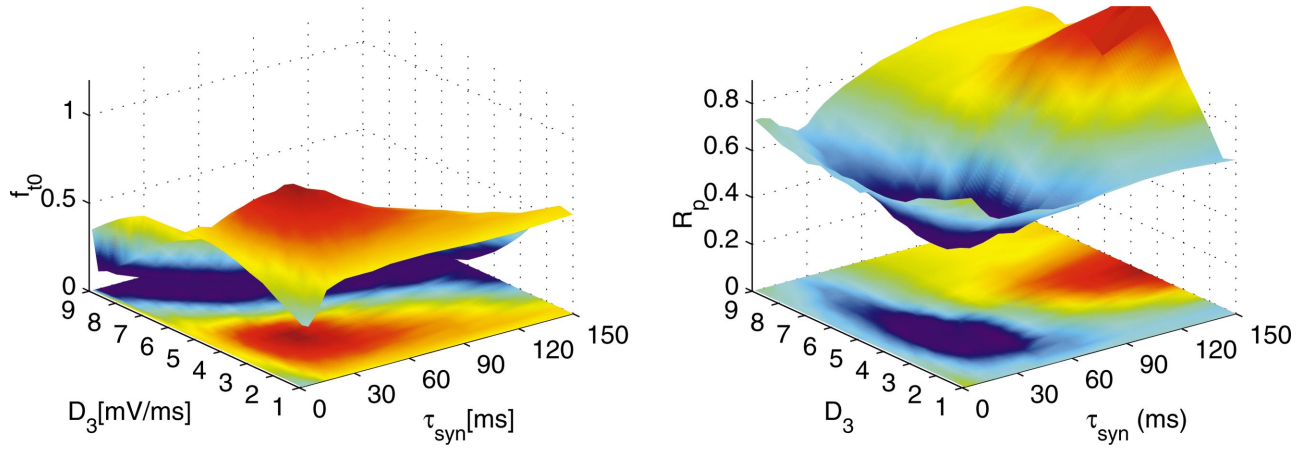

FIG. 6. (Color) Left: Fraction of pulses f_{t0} occurring at intervals T_p equal ($\pm 5\%$) to the period of the ghost resonance ($T_0=1/f_0$). Right: Coefficient of variation R_p. Both quantities plotted as function of noise amplitude (D_3) and τ_{syn}.

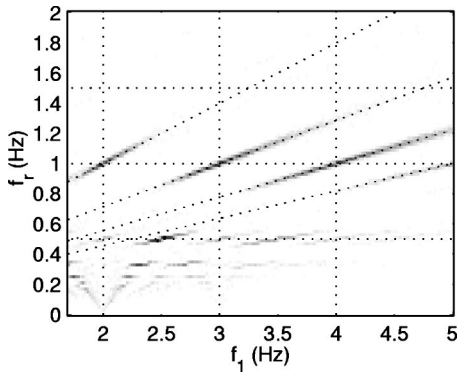

FIG. 7. Probability of observing a spike in the processing neuron with instantaneous rate f_r (in gray scale) as a function of the frequency f_1 of one of the input neurons. We can observe a remarkable agreement of the responses following the lines predicted by Eq. (12) for $k=2,3,4,5$ (dashed lines from top to bottom). Parameters: $\tau_{syn}=35$ ms, $g_{syn}=1.0$ nS, $D_3=4.0$ mV/ms, $f_1=2Hz+\Delta f$, $f_2=3Hz+\Delta f$.

nally harmonic components of the input are all shifted in frequency by a constant Δf. In such a way the individual component are still separated in frequency by a constant missing "fundamental" f_0, but are no longer multiples of it. The frequencies f_1 and f_2 are chosen to be

$$f_1 = kf_0 + \Delta f, \quad f_2 = (k+1)f_0 + \Delta f, \tag{11}$$

with k integer. In other words, f_0 is no longer the greatest common divider of f_1 and f_2, even though its still their difference. If the system is simply detecting the difference $f_2 - f_1$, it should always display a fixed resonance at f_0, independently of the frequency shift Δf. But if the pitch detection does depends on Δf, it will no longer be perceived as the difference between the input frequencies. This last situation is in fact what was found in human experiments.[11] The neural mechanism proposed in Refs. 7 and 8 shows that the frequency of the ghost resonance shifts linearly with Δf following the relation:

$$f_r = f_0 + \frac{\Delta f}{k+1/2}. \tag{12}$$

in agreement with the auditory experimental results of Refs. 9–11.

We now examine whether a scaling similar to that of Eq. (12) is observed in the response of the processing neuron. We fix the noise amplitude D_3 and synaptic time τ_{syn} to their optimal values at the resonance ($D_3=4$ mV/ms, $\tau_{syn}=35$ ms) and compute the probability of observing a spike with rate f_r for increasing Δf. The results are plotted in Fig. 7 as a function of f_1, and show that the largest probability corresponds to spike rates following the prediction of relation (12). Changing the noise amplitude only obscures the observation of the spike density, but it does not affect the agreement with the theoretical expression. In the bottom of Fig. 7 one can also see traces of less probable spikes, corresponding to a trivial subharmonic response of the system.

Figure 7 shows that the processing neuron emits spikes following Eq. (12) for $k=2,3,4,5$. As mentioned above, this relation is sustained by experimental data of pitch detection.[11] Those experimental results indicate that equidistant tones in monoaural presentation do not produce constant pitch, similarly to what we observe in our binaural numerical experiments. We are not aware of binaural human experiments shifting the frequency components as in Ref. 11, which would be interesting to compare with our numerical predictions in Eq. (12).

V. CONCLUSIONS

In this paper we demonstrate the phenomenon of ghost stochastic resonance in a neural circuit where two neurons receive two components of a complex signal and their outputs drive a third neuron that processes the information. The results show that the processing neuron responds preferentially at the "missing fundamental" frequency, and that this response is optimized by synaptic noise and by synaptic time constant. The processing neuron is able to detect the coincident arrival of spikes from each of the input neurons, and this coincidence detection is analogous to the linear interference of harmonic components responsible of the ghost response in the single-neuron case.[7] A brain structure candidate for this dynamics is the inferior colliculus, which receives multiple inputs from a host of more peripheral auditory nuclei. Details of the physiology of this nucleus are still uncertain, but enough evidence suggests that temporal and frequency representations of the inputs are present in the spike timing of their neurons. Our results suggest that the neurons in this nucleus can exhibit the dynamics described here, thus participating in the perception of binaural pitch. The main consequence of these observations is that pitch information can be extracted mono or binaurally via the same basic principle, i.e., ghost stochastic resonance, operating either at the periphery or at higher sensory levels.

ACKNOWLEDGMENTS

We thank Dante R. Chialvo for guidance and useful comments on the paper. We also thank Claudio Mirasso for helpful remarks, and two anonymous referees whose constructive criticisms have led to qualitative improvements in the manuscript. We acknowledge financial support from MCyT-FEDER (Spain, Project Nos. BFM2002-04369 and BFM2003-07850), and from the Generalitat de Catalunya. P.B. acknowledges financial support from the Fundación Antorchas (Argentina).

[1] P. Parmananda, C. H. Mena, and G. Baier, Phys. Rev. E **66**, 047202 (2002).
[2] C. R. Laing and A. Longtin, Phys. Rev. E **67**, 051928 (2003).
[3] A. Longtin and D. R. Chialvo, Phys. Rev. Lett. **81**, 4012 (1998).
[4] B. Lindner, J. García-Ojalvo, A. Neiman, and L. Schimansky-Geier, Phys. Rep. **392**, 321 (2004).
[5] E. Ullner, A. Zaikin, J. García-Ojalvo, R. Báscones, and J. Kurths, Phys. Lett. A **312**, 348 (2003).
[6] J. D. Victor and M. M. Conte, Visual Neurosci. **17**, 959 (2000).
[7] D. R. Chialvo, O. Calvo, D. L. Gonzalez, O. Piro, and G. V. Savino, Phys. Rev. E **65**, 050902(R) (2002).
[8] D. R. Chialvo, Chaos **13**, 1226 (2003).
[9] P. A. Cariani and B. Delgutte, J. Neurophysiol. **76**, 1698 (1996).
[10] P. A. Cariani and B. Delgutte, J. Neurophysiol. **76**, 1717 (1996).
[11] J. F. Schouten, R. J. Ritsma, and B. L. Cardozo, J. Acoust. Soc. Am. **34**, 1418 (1962).

[12]O. Calvo and D. R. Chialvo, "Ghost stochastic resonance on an electronic circuit," unpublished (2004).
[13]J. M. Buldú, D. R. Chialvo, C. R. Mirasso, M. C. Torrent, and J. García-Ojalvo, Europhys. Lett. **64**, 178 (2003).
[14]C. Pantev, T. Elbert, B. Ross, C. Eulitz, and E. Terhardt, Hear. Res. **100**, 164 (1996).
[15]E. C. Cramer and W. H. Huggins, J. Acoust. Soc. Am. **30**, 858 (1958).
[16]J. M. Buldú, C. M. González, J. Trull, M. C. Torrent, and J. García-Ojalvo, Chaos **15**, 013103 (2005).
[17]C. Morris and H. Lecar, Biophys. J. **35**, 193 (1981).
[18]M. St-Hilaire and A. Longtin, J. Comput. Neurosci. **16**, 299 (2004).
[19]P. Balenzuela and J. Garcia-Ojalvo (unpublished).
[20]K. Tsumoto, T. Yoshinaga, K. Ahiara, and H. Kawakami, in *Proc. International Symposium on Nonlinear Theory and its Applications* 1, 363 (2002).
[21]A. Destexhe, Z. F. Mainen, and T. J. Sejnowski, Neural Comput. **6**, 14 (1994).
[22]J. García-Ojalvo and J. M. Sancho, *Noise in Spatially Extended Systems* (Springer, New York, 1999).
[23]A. Longtin, J. Stat. Phys. **70**, 309 (1993).